FEBS Letters

FEBS PRESS science publishing by scientists

Expression of the translation termination factor eRF1 is autoregulated by translational readthrough and 3'UTR intron-mediated NMD in *Neurospora crassa*

Anita Kurilla[1], Anita Szőke[2], Andor Auber[1], Krisztina Káldi[2] and Dániel Silhavy[1,3]

1 Department of Genetics, NARIC, Agricultural Biotechnology Institute, Gödöllő, Hungary
2 Department of Physiology, Faculty of Medicine, Semmelweis University, Budapest, Hungary
3 Biological Research Centre, Institute of Plant Biology, Szeged, Hungary

Correspondence
D. Silhavy, Biological Research Centre, Institute of Plant Biology, Temesvári krt 62, H-6726, Szeged, Hungary
Tel: 36 30 760 34 26
E-mail: silhavy@brc.hu

(Received 21 May 2020, revised 30 July 2020, accepted 17 August 2020, available online 12 September 2020)

doi:10.1002/1873-3468.13918

Edited by Claus Azzalin

Eukaryotic release factor 1 (eRF1) is a translation termination factor that binds to the ribosome at stop codons. The expression of eRF1 is strictly controlled, since its concentration defines termination efficiency and frequency of translational readthrough. Here, we show that eRF1 expression in *Neurospora crassa* is controlled by an autoregulatory circuit that depends on the specific 3'UTR structure of *erf1* mRNA. The stop codon context of *erf1* promotes readthrough that protects the mRNA from its 3'UTR-induced nonsense-mediated mRNA decay (NMD). High eRF1 concentration leads to inefficient readthrough, thereby allowing NMD-mediated *erf1* degradation. We propose that eRF1 expression is controlled by similar autoregulatory circuits in many fungi and seed plants and discuss the evolution of autoregulatory systems of different translation termination factors.

Keywords: autoregulation; convergent evolution; eukaryotic Release Factor 1; nonsense-mediated decay; readthrough; translation termination

When a ribosome reaches a stop codon, the eukaryotic release factor 1 (eRF1) binds to the A site and with the help of eukaryotic release factor 3 (eRF3) terminates translation. If a transcript contains specific signals and/or the cellular conditions do not favor normal translation termination, alternative events such as readthrough or nonsense-mediated decay (NMD) can occur at the stop codon [1,2].

Readthrough occurs if a tRNA binds to the stop codon and translation is continued till the next in-frame stop codon (referred to as 'next stop' throughout this manuscript) [3]. Readthrough produces C terminally extended protein forms that can function differently from the normal protein version [4–6]. Moreover, at least in fungi, readthrough is involved in adaptation and evolvability [7]. Readthrough frequency depends mainly on the sequence context of the stop codon and on the level of proteins involved in termination such as eRF1 (sees below). The stop-CARYYA sequence is the most typical readthrough promoting signal in eukaryotes [8]. The + 4C, the first nucleotide downstream of the stop codon, is the most important readthrough stimulating element [9].

NMD is a translation termination coupled eukaryotic quality control system that identifies and rapidly degrades premature termination codon containing aberrant mRNAs and controls the expression of several normal transcripts. It might also facilitate adaptive evolution [10]. NMD is induced when the translation termination is inefficient because the termination stimulating 3'UTR signals are absent and/or termination inhibitory signals are present in the 3'UTR. Unusually

Abbreviations
3'UTR, 3' untranslated region; EJC, exon–junction complex; eRF1, eukaryotic release factor 1; NMD, nonsense-mediated decay; RT, readthrough; RT-NMD 3'UTR, readthrough-nonsense-mediated decay 3' untranslated region; uORF, upstream open reading frame.

FEBS Letters **594** (2020) 3504–3517 © 2020 The Authors. *FEBS Letters* published by John Wiley & Sons Ltd on behalf of Federation of European Biochemical Societies

long 3'UTRs and introns located > 50 nt downstream of the stop codon are the NMD-inducing signals [11]. The key NMD factor up-frameshift 1 (UPF1) is an RNA-dependent helicase and ATPase that binds to mRNAs including the 3' untranslated regions [12]. Long 3'UTR induces NMD because it inhibits the binding of the poly(A) binding protein (PABP) to the eRF3. Thus, eRF3 can recruit UPF1 to the terminating ribosome, and then, UPF1 is bound by the UPF2 and UPF3 proteins and the UPF1-2-3 NMD complex triggers the rapid decay of the mRNA. 3'UTR located introns can also induce NMD (this branch of NMD is referred to as EJC-dependent NMD). In certain eukaryotes including vertebrates, plants, and *Neurospora crassa*, splicing results in the deposition of a protein complex (called exon–junction complex, EJC) onto the mRNA 20-24 nt upstream of the new exon–exon boundary [13–15]. The EJC is a binding platform for the UPF3 and UPF2 NMD factors. During translation, the ribosome displaces the EJCs and UPF1s from the 5'UTR, the coding region and the first 20-25 nt of the 3'UTR, but fails to remove from the 3'UTR [16,17]. These 3'UTR EJCs trigger NMD efficiently presumably by increasing the local concentration of UPF3 and UPF2. It was shown that in *N. crassa*, the 3'UTR located introns can trigger EJC-dependent NMD [14,18]. It was also demonstrated that the UPF1, UPF2 and UPF3 NMD factors, the eIF4A3, Y14, and Magoh EJC components and the pioneer translation specific cap-binding (CBC20 and CBC80) proteins are required for the EJC-dependent NMD in *N. crassa*. Upstream ORFs (uORF) present in the 5'UTR of mRNAs can also activate NMD in *N. crassa* although the mechanistic basis of uORF triggered NMD is not known. NMD is regulated by various autoregulatory circuits in different eukaryotes. In *N. crassa*, *eif4a3* and *y14* mRNAs contain a 3'UTR intron and are targets of the EJC-dependent NMD. *upf1* mRNA is also targeted by NMD in *N. crassa* despite it does not contain intron in the 3'UTR [14].

All three events, translation termination, readthrough, and NMD, are physiologically important and interconnected. It was shown that a certain level of readthrough is required for viability in yeast and *Drosophila* [4,6]. NMD deficiency is lethal in vertebrates and plants and leads to reduced growth in *N. crassa* and yeast [14,19,20]. eRF1 concentration is critical for keeping the balance between these events [21,22]. Low eRF1 protein level reduces termination efficiency, thereby increasing the frequency of readthrough, while eRF1 overexpression reduces readthrough frequency below a critical level and could lead to premature termination at rare codons [23,24]. In plants, eRF1 overexpression also intensifies NMD via an unknown mechanism [22]. Thus, eRF1 expression has to be strictly regulated. Indeed, altered eRF1 concentration leads to growth phenotype and strong selection acts to maintain optimal termination efficiency in different yeast strains [7,25]. eRF1 and near cognate tRNAs compete for the stop codon, and hence, low termination efficiency leads to enhanced readthrough. Moreover, in yeast, mammals and plants, readthrough can protect mRNAs that contain NMD-activating elements in their 3'UTR from NMD if the stop codon of the ORF is in a readthrough context and the next stop is not in an NMD-inducing position [22,26–28]. It is postulated that when readthrough occurs at the stop codon, the translating ribosome removes NMD stimulatory signals including EJCs from the 3'UTR region till the next stop codon, thereby rescuing the mRNA from NMD [22,28].

Previously, we have demonstrated that in plants eRF1 is controlled by a complex autoregulatory circuit in which both readthrough and NMD are involved [22]. In higher plants, *eRF1* is always present in multiple copies, and one of the *eRF1* copies (*eRF1-1*) has a specific 3'UTR structure (Fig. 1A) called Readthrough-NMD (RT-NMD) structure [22], [29–31]. The RT-NMD structure of *eRF1-1* mRNA has three critical elements: (i) the stop codon context of *eRF1-1* mRNA facilitates readthrough, (ii) *eRF1-1* has an intron in the 3'UTR that can activate EJC-dependent NMD (referred to as NMD intron), and (iii) the next stop of *eRF1-1* is not in EJC-dependent NMD-inducing position (it is located downstream or closer than 50 nt to the intron). We found that in *A. thaliana*, *eRF1-1* is the only transcript that has RT-NMD structure and that this unique structure is required for the eRF1 autoregulation. *eRF1-1* mRNA is targeted by NMD and the readthrough partially rescues the *eRF1-1* transcript from it. If eRF1 protein level is unusually high, the frequency of readthrough is reduced and NMD targets more efficiently the *eRF1-1* mRNA. Thus eRF1-1 protein production and consequently the total eRF1 protein concentration is reduced [22]. As it was shown that in *N. crassa eRF1* is a single copy gene that has an NMD-inducing intron in the 3'UTR [14], we hypothesized that *N. crassa erf1* mRNA, like plant *eRF1-1* transcript, has an RT-NMD structure and it is also autoregulated. We show that *N. crassa erf1* has a functional RT-NMD 3'UTR, its 3'UTR induces NMD while the readthrough partially protects the transcript from NMD. We also found that *N. crassa erf1* is autoregulated, overexpression of eRF1 leads to reduced endogenous *erf1* mRNA level. Our finding that *erf1* overexpression without the autoregulatory RT-NMD 3'UTR structure leads to slightly slower growth supports the assumption that eRF1

autoregulation is physiologically relevant. Furthermore, we demonstrate that unusually long 3'UTR can activate NMD in *N. crassa* and that it plays a role in NMD autoregulation by targeting the mRNA of key NMD factor UPF1. The evolution of different translation termination factor autoregulatory systems will be discussed.

Materials and Methods

Strains

FGSC #2489 (74-OR23-1VA, wild-type), FGSC#11229 (NCU04242, *Δupf1*), FGSC#15706 (NCU05267, *Δupf2*), FGSC #11679 (NCU03435, *Δupf3*), and the FGSC#6103 (1-234-723) *Δhis-3 N. crassa* strains were obtained from the Fungal Genetics Stock Center (FGSC). The his-3 marker was introduced into the *Δupf1* strains by crossing FGSC#6103 (his-3, mat A) with FGSC#11229 (mat a). The strains used in this study are listed at Table S1.

Plasmid construction and transformation

Vectors and primers used in this study are listed at Table S1, and the details of cloning are described in Supplementary Material and Methods. pCCG3XFLAG and pMF270 vectors were obtained from the FGSC. Codon-optimized firefly *luciferase* was amplified from the pBM60-Pfrq-luc-trpC [32] vector and cloned with BamHI and SpeI into pCCGN3XFLAG vector (pAK01). Different *luc.* reporter plasmids were generated by incorporating the various stop codon context-terminator regions into pAK01. *eRF1-* and *Dom34*-overexpressing plasmids were generated in pMF270 backbone (for details, see Appendix S1). Plasmids were linearized with NdeI and integrated into the his-3 locus of wild-type (*wt*) or *Δupf1* by electroporation performed with a BTX Electro Cell Manipulator 600 (2,1 kV, 25 μF, 480 Ω).

Culture conditions

Conidia were obtained from cultures grown in 100-mL Erlenmeyer flasks containing 25 mL VM/2% sucrose/2% agar [33]. Cultures were grown at 25 °C, 12 : 12 h L : D for 7 days in a growth chamber (Forma Diurnal Growth Chamber, Thermo Fisher Scientific, Corston, Bath, UK). Conidia were washed with 20 mL VM/2% sucrose and filtered through cheesecloth. Conidial concentration was counted with a hemacytometer. 2×10^8 conidia were inoculated into 25 mL VM/2% sucrose and germinated at 30°C/LL for 6 h with 150 rpm shaking. Cells were harvested with vacuum filtration onto Whatman 541 filter paper, and then, the paper was washed with 4 °C sterile

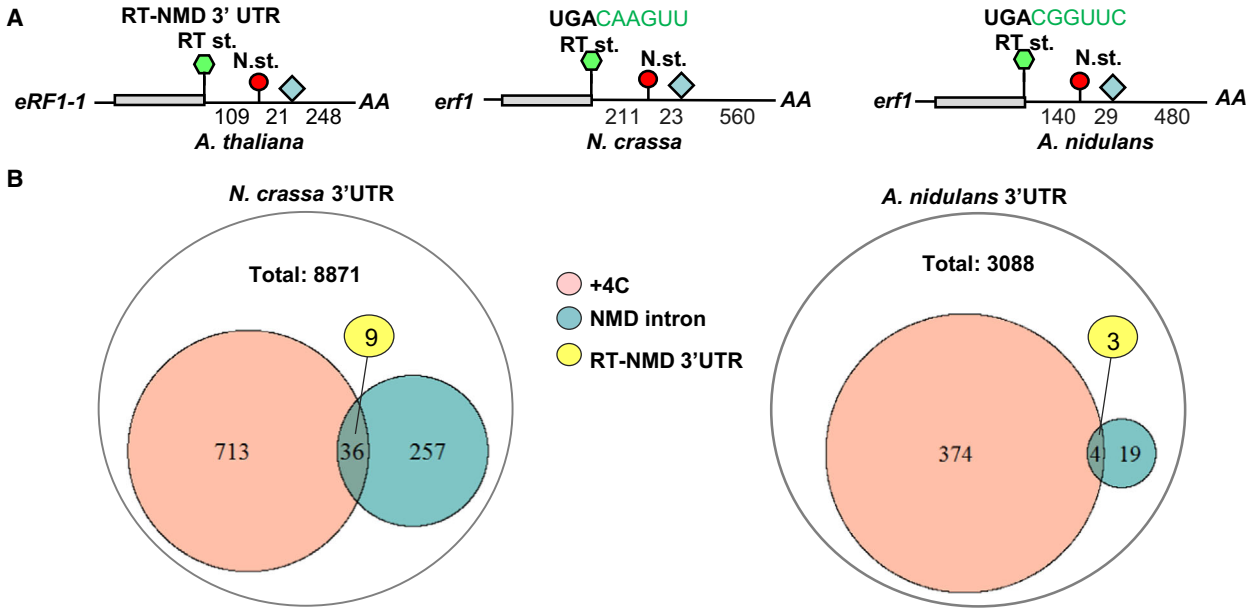

Fig. 1. The *N. crassa erf1* mRNA has a functional RT-NMD 3'UTR. (A) Schematic, nonproportional representation of *Arabidopsis eRF1-1*, *N. crassa erf1*, and *A. nidulans erf1* mRNAs. Green hexagon shows stop codon in readthrough (RT st.) context. The next stop (N. st.), which is not in a readthrough context, is represented as a red circle. The 3'UTR intron is shown as a pale blue diamond. Numbers indicate the distance in nucleotides. (B) The RT-NMD 3'UTR structure is very rare in *N. crassa* and *A. nidulans*. The annotated 3'UTRs of *N. crassa* and *A. nidulans*. The RT-NMD structure is defined as the intron is at least 50 nt downstream from the stop codon (NMD intron), the stop codon is in a readthrough promoting context (+4 is C), and the next stop located downstream or is closer than 50 nt to the intron.

water and cut into ~ 0,1 g pieces. The samples were quickly frozen in liquid nitrogen and stored at −70 °C until RNA or protein isolation.

Phenotypic analyses and measurement of growth rate

For phenotypic analyses, *N. crassa* strains were grown on VM slant tubes (VM, 2% glucose, 2% agar, 0,05% biotin) at 25 °C, 12 : 12 h L:D for 7 days in a growth chamber (Forma Diurnal Growth Chamber, Thermo Fisher Scientific). The growth rate was measured in race tube assay. Cultures were inoculated onto standard race tube media (VM, 3.2% agar, 0,17% arginine, 0,05% biotin) or media supplemented with 4% NaCl, or the indicated amount (75 μM, 100 μM) of menadione. Race tubes were incubated at 25 °C or for the NaCl assay at 30 °C, in constant light (Infors HT Minitron, Ser.Nr.:#111033). Growth rates were calculated by distance grown and time elapsed ($mm \cdot min^{-1}$).

DNA isolation and selection of homokaryotic transformants

Genomic DNA was extracted from conidia as described [34]. PCR amplification from genomic DNA was conducted with MyTaq Red DNA polymerase (2x) (Izinta). Homokaryotic isolates were obtained by microconidiation and confirmed by PCR with *HisFor* and *HisRev* homokaryon-specific primers (Table S1). A ~ 200 nt fragment is amplified from heterokaryotic strains, but no fragment is amplified from homokaryons. *eRF1For* and *eRF1Rev* primers were used to confirm template quality.

RNA isolation and qRT-PCR

Total RNA was isolated as described [35] with Trizolate reagent. Following the DNAse treatment (DNAse, Fermentas, Thermo Fischer Scientific, Waltham, MA, USA), cDNA was synthesized from 200 ng of total RNA using Revertaid Reverse Transcription Kit (Thermo Scientific). Transcript levels were quantified by quantitative real-time PCR (qPCR) with Fast Start Essential DNA Green Master Mix (Roche, Basel, Switzerland) in a Light Cycler 96 Real-Time PCR instrument (Roche). The quantification was relative to *vmaI* mRNA level. Primers used for qRT-PCR assays are listed in Table S1.

Luciferase assays

Protein extracts were prepared as described [35]. Protein concentration of the extracts and the BSA standards was determined by Bradford assay [36]. Absorbance was measured with Eppendorf Biophotometer at OD 595. Luciferase activity measurements were performed in a Chameleon microplate reader (Hidex) by mixing 10 μL of protein extract (diluted to 10 $ng \cdot \mu L^{-1}$) and 10 μL firefly luciferase assay reagent (25 mM glycylglycine, 15 mM potassium phosphate solution pH 8.0, 15 mM MgSO4, 4 mM EGTA, 2mM ATP, 1 mM DTT, 0.1 mM CoA, and 0.075 mM luciferin) [37]. Luciferase activity was normalized to protein amount.

Statistics and Bioinformatics

Comparisons between groups were done by ANOVA and Tukey's test or Wilcoxon test to determine *P*-values. The *P*-values were calculated in R Statistical Environment. Statistical significance was set at $*P < 0.05$, $**P < 0.01$, and $***P < 0.001$. Venn diagram was made in R Statistical Environment.

JGI MycoCosm [38] and EnsemblFungi [39] databases were used to collect *erf1* or *dom34* transcripts from fungi. *N. crassa* transcript analysis was made by using JGI Mycocosm database. The *Δupf1* RNA-seq data sets were obtained from the GEO database (GSE97157) [18]. RNA logos were created with WebLogo software from 122 fungal mRNAs [40].

Results

N. crassa erf1 mRNA has a potential RT-NMD 3'UTR structure

Plant eRF1-1 mRNA has an RT-NMD 3'UTR structure, it contains an NMD intron in the 3'UTR, a stop codon in a readthrough-stimulating context and a next stop, which is not in an EJC-dependent NMD-inducing position (Fig. 1A left panel). This unique 3'UTR structure allows autoregulation of plant eRF1 [22]. It was reported that the *N. crassa erf1* mRNA also harbors an EJC-dependent NMD-inducing intron in its 3'UTR (234 nt downstream from the stop codon). In line, *erf1* is overexpressed in NMD mutants [14] (Fig. S1). To assess whether *N. crassa erf1* mRNA has a potential RT-NMD structure, we studied the stop codon context and the position of the next stop. We found that the stop codon is in a potentially efficient RT context as the + 4 is C and the sequence downstream of the stop codon deviates only slightly from the canonical RT context (consensus RT context C^{+4}ARYYA, *N. crassa* potential RT context C^{+4}AAGTT). Moreover, the *erf1* mRNA has an UGA stop codon, known to allow the highest readthrough frequency (Fig. 1A middle panel) [2,9]. The next stop of *N. crassa erf1* is only 23 nt upstream to the 3'UTR intron, and thus, it is not in an EJC-dependent NMD-inducing position. These data show that the *N. crassa erf1* mRNA has a potential RT-NMD 3'UTR

structure. This 3'UTR structure (defined as containing an intron> 50 nt from the stop, the stop context has a + 4 C, and the next stop is downstream or closer than 50 nt to the intron) is rather uncommon in *N. crassa* (Fig. 1B), only 9 mRNAs (out of 8871 *N. crassa* genes having annotated 3'UTR) have an RT-NMD 3'UTR structure. Based on our data that (i) the eRF1 mRNAs have RT-NMD 3'UTR structure in plants as well as in *N. crassa* even though that this structure is very rare in these organisms, and that (ii) in plants, RT-NMD 3'UTR structure plays a critical role in eRF1 autoregulation, we assumed that the RT-NMD 3'UTR structure of *erf1* mRNA is also physiologically important in *N. crassa*.

Readthrough partially protects the *N. crassa erf1* mRNA from its 3'UTR intron-induced NMD

In plants, readthrough partially rescues the *eRF1-1* mRNA from its 3'UTR intron-induced NMD. To test whether the readthrough stop codon context also alters the NMD sensitivity of *erf1* transcript, three *ccg1* promoter-driven *luciferase (luc)* reporter constructs having *erf1* 3'UTR with different stop codon context (Fig. 2A) were generated. The constructs were integrated into the *his-3* locus of wild-type and UPF1 mutant (*Δupf1*) *N. crassa* strains, and then, their expressions were compared. At the first construct, the *luc* was fused to the stop and terminator region of *N. crassa* eRF1 gene (*L-RTst* for *Luciferase* with *eRF1* Readthrough Stop context and *eRF1* 3'UTR/Terminator). The *L-RTst* mRNA level was ~ 2 times higher in the NMD-deficient *Δupf1* than in the wild-type strain. In line, the Luc. activity was also ~ 2-fold more intense in the *Δupf1* strain (Fig. 2B). These data confirmed previous results (obtained with a similar reporter controlled by *cox-5* promoter) that the 3'UTR of *erf1* induces NMD [14] and suggested that *erf1* readthrough stop context cannot completely protect the transcript from the 3'UTR activated NMD. To test whether the readthrough stop context can partially protect the transcript from NMD, the + 4 C of the *L-RTst* construct was modified to G (*L-C/Gst*). It is known that replacing the + 4 C with G dramatically reduces the readthrough frequency [2]. We assumed that if readthrough context partially protects the mRNA from NMD, the *L-C/Gst* reporter mRNA will be more sensitive to NMD than the *L-RTst* transcript. Indeed, in the wild-type background, the + 4 C to G change led to reduced reporter mRNA level and weaker Luc. activity (Fig. 2C left panels, compare column 1 to 2). In contrast, the *L-C/Gst* and *L-RTst* reporter transcripts expressed similarly in the NMD-deficient *Δupf1* background (Fig. 2C right panels). These data suggest that in *N. crassa* readthrough partially rescues the *erf1* mRNA from its 3'UTR-induced NMD. In plants, readthrough can only protect the transcript from the 3'UTR intron-induced NMD if the next stop is not in an NMD-inducing position. To test whether it is also essential for NMD rescue in *N. crassa*, a third reporter construct was generated in which an in-frame stop codon was inserted 9 nt downstream from the normal stop (*L-ststst*). This artificial next stop is still in an EJC-dependent NMD-inducing position. In the *wt* background, the *L-ststst* reporter mRNA was expressed at significantly lower level than the *L-RTst* control transcript, while the two reporters had similar expression levels in the *Δupf1* strain (Fig. 2C). These data suggest that readthrough can protect *erf1* mRNA from NMD only if the next stop is not in an NMD-inducing position. To directly confirm that the next stop of *erf1* is not in an NMD-activating position, an additional reporter construct was generated (*L-nxst*) by replacing the stop codon with a coding codon, and thus, translation terminates at the (original) next stop. As expected, the *L-nxst* was not targeted by NMD, and the reporter transcript was expressed at enhanced levels relative to the *L-RTst* control mRNA in the *wt* background, while the two transcripts accumulated to comparable levels in the *Δupf1* strain (Fig. 2D).

To exclude that the expressional differences are due to different splicing efficiency, we compared the splicing of the reporter transcripts. RT-PCR experiments showed that the 3'UTR intron was efficiently spliced from all reporter mRNAs in both wild-type and *Δupf1* backgrounds (Fig. 2E).

Taken together, these results show that the RT-NMD 3'UTR structure functions similarly in plants and *N. crassa*, the readthrough can partially rescue the *erf1* mRNA from the 3'UTR intron-induced NMD when the next stop is not in an NMD-inducing position.

N. crassa eRF1 is autoregulated, overexpression of eRF1 leads to reduced endogenous *erf1* mRNA level

As the RT-NMD 3'UTR structure of eRF1 transcript allows autoregulation in plants [22], we assumed that the RT-NMD structure of *erf1* mRNA also allows autoregulation in *N. crassa*. To address this issue, an eRF1-overexpressing strain was generated (eRF1oe), in which the eRF1 coding region was cloned between the *ccg1* promoter and the *ADH1* terminator into the *his3* site (Fig. 3A). A nontransgenic strain and a

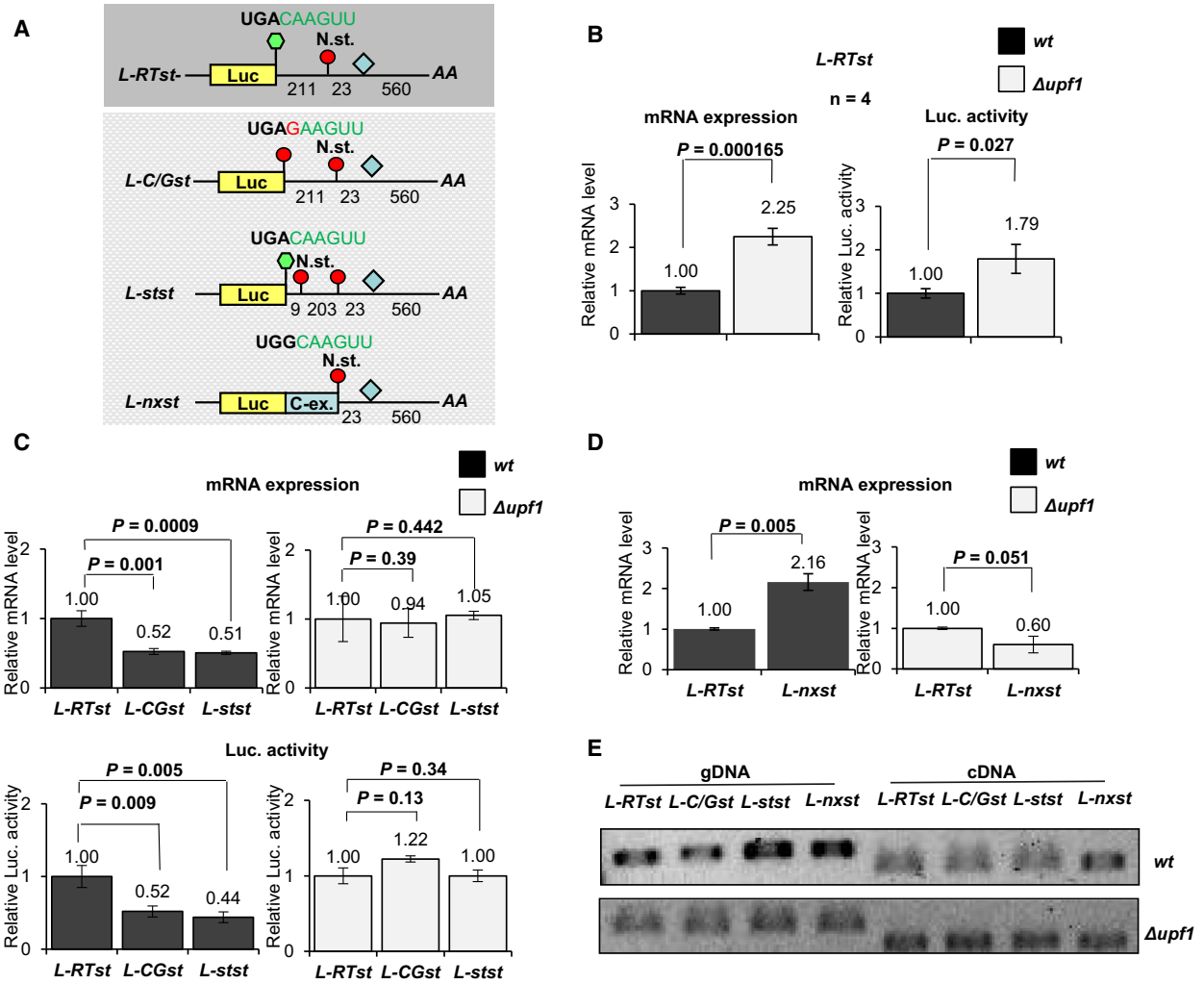

Fig. 2. Readthrough partially rescues the transcript from *erf1* 3′UTR-induced NMD in *N. crassa*. (A) Schematic, nonproportional representation of the reporter transcripts used in this experiment. Codon-optimized luciferase reporter (Luc) is fused to the RT-NMD 3′UTR of *erf1* (*L-Rtst*) or to the modified versions of this 3′UTR in which the readthrough stop codon context is mutated (*L-C/Gst*) or an artificial next stop is incorporated (*L-stst*) or the stop codon is changed to a coding codon (*L-nxst*). C-ex. represents the C-terminal extension. Green hexagon shows stop codon in readthrough (RT st.) context and red circle represents a stop codon in nonreadthrough context. N. st. marks the next stop. The 3′UTR intron is shown as a pale blue diamond. Numbers indicate the distance in nucleotides. (B) *erf1* 3′UTR activates NMD. *L-Rtst is* expressed in wild-type (*wt*) and *Δupf1* backgrounds (black and gray columns, respectively). Reporter mRNA levels (mRNA expression) and fluorescence (Luc. activity) were measured. Average values of four independent samples ($n = 4$) were calculated, and then, the *wt* average was taken as 1 and the other average values were normalized to it. Data are represented as means ± SD. (C) Readthrough partially rescues *erf1* RT-NMD 3′UTR containing transcripts from NMD in *N. crassa*. *L-C/Gst* and *L-stst* test and *L-Rtst* control transcripts were expressed in *wt* and *Δupf1* backgrounds (left and right panels, respectively), and mRNA expression and Luc. activity were measured (upper and bottom panels). (D) The next stop of *erf1* is not in an NMD-inducing position. (E) The *erf1* 3′UTR intron is efficiently spliced. RT-PCR shows (cDNA) that the intron is comparable spliced from each reporter in both backgrounds. PCR from genomic DNA(gDNA) with the same primers was used as control. Wilcoxon (2B and D) or Tukey's (2C) statistical test was used.

transgenic strain, in which the Luc was targeted to the same position, were used as controls (Fig. 3A). We found that the total *erf1* mRNA (transgenic + endogenous *erf1* mRNAs) level was very similar in the wild-type and Luc transgenic strains, while it was significantly increased in the eRF1oe strain. Moreover, the level of the endogenous *erf1* transcript was moderately but significantly reduced relative to the wild-type in the eRF1oe but not in the Luc transgenic strains (Fig. 3B). Two independent transformants were analyzed with similar results (Fig. S2) We have also tested whether overexpression of the eRF1 paralog *Dom34*

can modify the *erf1* level. As Fig. 3C shows, Dom34 overexpression (Dom34oe) did not alter the *erf1* mRNA level. In contrast, the *dom34* mRNA expression was reduced in the eRF1oe strain, suggesting that via an unknown mechanism eRF1 protein inhibits the expression of its paralog.

These findings showing that eRF1 (but not Luc or Dom34) overexpression led to lower endogenous *erf1* mRNA level suggests that eRF1 is autoregulated in *N. crassa*. Alternatively, eRF1 overexpression intensifies NMD and decreases the expression of all EJC-dependent NMD targets. To distinguish between these possibilities, we measured the expression of *eif4a3* EJC-dependent NMD target (Fig. S1). *eif4a3* expression was not modified in the eRF1oe strain (Fig. 3B right panel), suggesting that eRF1 overexpression selectively reduced *erf1* level. To further support our results, we generated a transgenic strain in which the genomic copy of *N. crassa eRF1* gene was targeted into the *his-3* position (eRF1oe2). To measure independently the transgenic and endogenous *erf1* mRNAs, a 200 nt segment was deleted from the 5' UTR region of the transgenic copy (Fig. 3D). Relevantly, unlike the previously used *erf1oe* transgenic mRNA, the *erf1oe2* mRNA has an RT-NMD 3'UTR. As in the *erf1oe2* strain, both the transgenic and the endogenous *erf1* transcripts are sensitive to the eRF1 protein level, we expected that the total *erf1* level will be barely (if at all) enhanced and that the endogenous *erf1* mRNA expression will be only slightly reduced. Indeed, we found that the endogenous *erf1* mRNA level was slightly but significantly reduced in the *eRF1oe2* transgenic strain, while

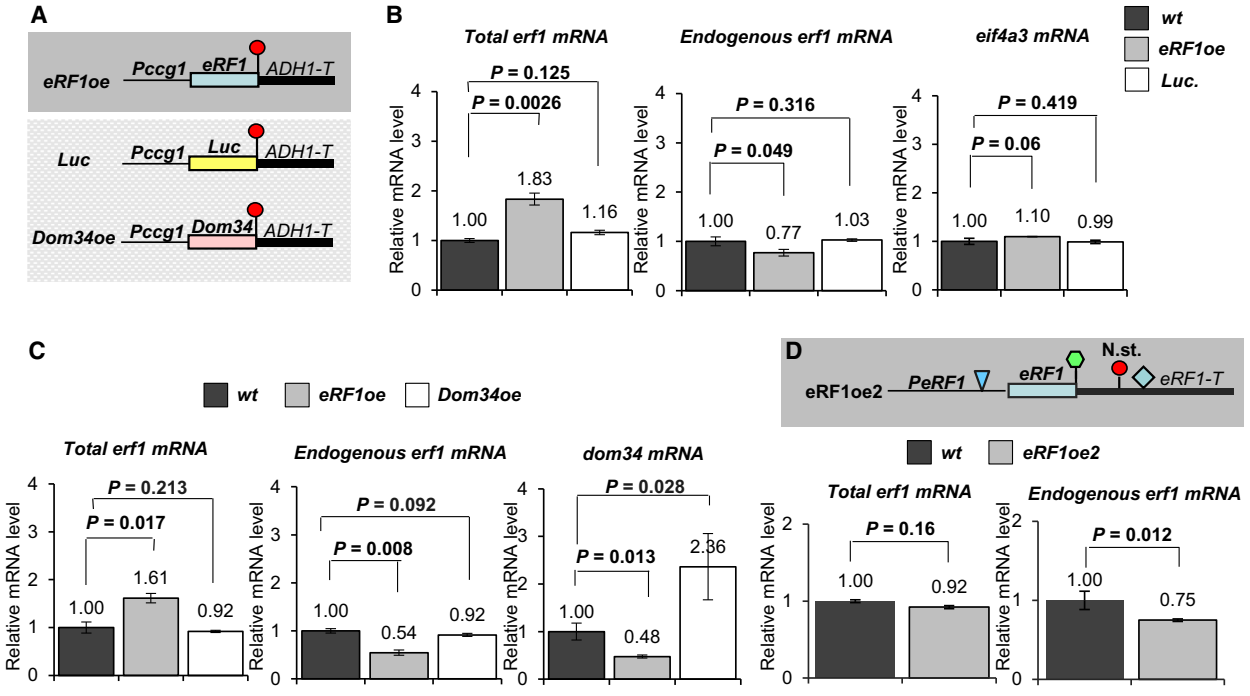

Fig. 3. eRF1 is autoregulated in *N. crassa*. (A) Schematic, nonproportional representation of the constructs used in this experiment. Codon-optimized luciferase reporter (*Luc*), *N. crassa eRF1* (*eRF1oe*), and *Dom34* (*Dom34*oe) genes were fused to the terminator region of *ADH* (ADH-T). The ccg1 promoter (P-ccg1) regulates the transcription. Red circle represents stop codon in nonreadthrough context. (B-D) The eRF1 is autoregulated. (B) eRF1 overexpression leads to reduced *erf1* mRNA level. qRT-PCR assays were conducted to measure the total (endogenous + transgenic) and the endogenous *erf1* and the *eif4a3* mRNA levels in nontransgenic (*wt*), eRF1-overexpressing (*eRF1oe*), and *Luc* transgenic *N. crassa* strains (black, gray, and dark gray columns, respectively). (C) Overexpression of the Dom34 does not lead to reduced *erf1* level. Total and endogenous *erf1* and *dom34* transcript levels were measured in *wt*, *eRF1oe*-, and *Dom34oe*-overexpressing strains. Note that the overexpression of Dom34 does not modify the *erf1* level, while eRF1 overexpression reduces the *dom34* mRNA level showing that eRF1 regulates the expression of the Dom34 paralog. (D) Transgenic expression of the genomic eRF1 copy (*eRF1oe2*) leads to reduced endogenous mRNA level. The construct contains the promoter (p-eRF1), the coding (eRF1), and the terminator (eRF1-T) regions of the *N. crassa* eRF1 gene. Green hexagon and red circle show stop codon in readthrough and nonreadthrough context, respectively. N. st. marks the Next stop. The 3'UTR intron is shown as a pale blue diamond. Blue triangle shows a short segment that is deleted from the 5'UTR region to allow selective PCR detection of transgenic and endogenous *erf1* transcripts. mRNA expressions and Luc. activities were calculated and shown as described at Fig. 2B. Wilcoxon (3 D) or Tukey's (3B and C) statistical test was used.

the total *erf1* mRNA was not altered (Fig. 3D). It is likely that the autoregulation controls the expression of both transgenic and endogenous *erf1* transcripts, and thus, it can keep the total *erf1* level close to wild-type level. In contrast, in the *eRF1oe* strain, the transgenic transcript is not regulated by the eRF1 protein. Therefore, the eRF1oe transgene can express more intensively thereby repressing more effectively the endogenous *erf1* levels.

Our data clearly suggest that eRF1 is autoregulated in *N. crassa*. As plant eRF1 autoregulation is based on the RT-NMD 3'UTR structure of eRF1-1 mRNA, and because the *N. crassa erf1* transcript also harbors an RT-NMD 3'UTR and shows autoregulation, we propose that the eRF1 autoregulation acts similarly in plants and *N. crassa*. Based on these data, we propose a model (Fig. 4A) in which high eRF1 protein level reduces the frequency of readthrough, and thus, the NMD can target more efficiently the autoregulated *erf1* transcripts. As a result, the reduced *erf1* mRNA expression leads to lower expression of the eRF1 protein (Fig. 4A).

In yeast, even slight over or underexpression of eRF1 (<2x) results in altered protein synthesis and modified growth [25]. To test whether moderate overexpression of eRF1 also results in modified growth in *N. crassa*, we compared the growth of wild-type and the *eRF1oe* and *eRF1oe2* transgenic strains (Fig. S3A, B). As the total *erf1* mRNA level was increased in the *eRF1oe* strain in which the transgenic *erf1* mRNAs are not autoregulated, but not in the *eRF1oe2* strain, in which the transgenic *erf1* transcripts are autoregulated (Fig. 3), we assume that the total eRF1 protein level is slightly enhanced in the *eRF1oe* strain relative to both wild-type and *eRF1oe2* strains. We found that growth of the *eRF1oe* strain was slightly retarded, and in race tube assays, its growth rate was moderately but significantly lower than the wild-type or the *eRF1oe2* transgenic strain (Fig. S3B). As the total *erf1* mRNA level was only slightly higher in the *eRF1oe* strain (1.5–1.8 X), the small differences are not surprising. Under salt (4%NaCl) stress condition the reduced growth of *eRF1oe* strain relative to the wild-type was more pronounced. The effect was especially strong at the first day (Fig. S3C). In contrast, *eRF1oe* strain grew comparably or even slightly better than the wild-type when ROS-inducing menadione treatment was applied (Fig. S3D). These data that *eRF1oe* strain grows more slowly than the wild-type under normal and salt stressed conditions support that in *N. crassa*, even moderately enhanced eRF1 level is slightly detrimental and suggest that *erf1* autoregulation can prevent

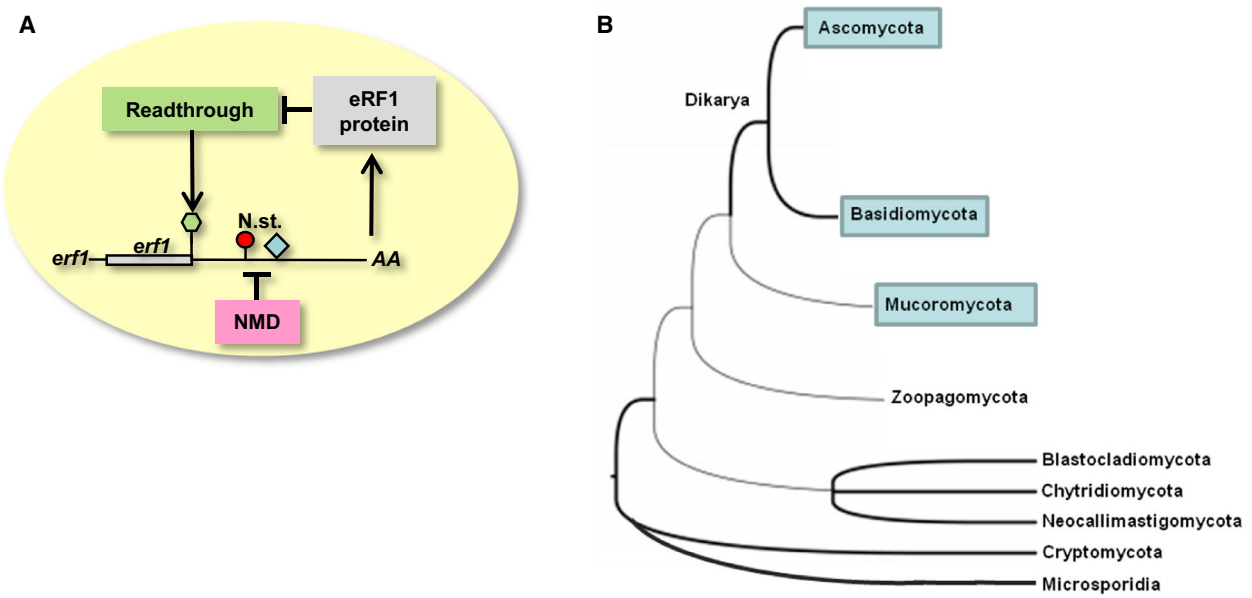

Fig. 4. Eukaryotic release factor 1 autoregulation was present in the common ancestor Mucoromycota and Dikarya. (A) Model of the eRF1 autoregulation in *N. crassa*. eRF1 protein reduces the frequency of readthrough at the *erf1* stop, and thus, NMD targets the *erf1* mRNA more efficiently and reduces the eRF1 protein level. (B) *erf1* RT-NMD 3'UTR structure in fungi. Tree was modified and redrawn from JGI MycoCosm and Nagy et al. (2017). JGI mycocosm tree represents the relationship between major groups of fungi. Thick branches represent well-known relationship, and thin branches mark uncertainties in our understanding of fungal relationships. The phyla, in which *erf1* transcripts with RT-NMD 3'UTR structure were found, are blue boxed.

overaccumulation of the termination factor. Thus in *N. crassa*, eRF1 autoregulation plays an important role in keeping the eRF1 concentration close to the optimal level.

eRF1 RT-NMD 3'UTR structure was already present in the ancestor of Dikarya and Mucoromycota fungi

To understand the evolution of eRF1 autoregulation in fungi, we studied the 3'UTRs of 124 annotated fungal *eRF1* genes from 27 fungal groups (class, subphyla or phyla) (Fig. S5. and Table S2). We found that 28 transcripts (in 10 classes) have NMD intron in their 3'UTRs and 49 mRNAs have + 4 C features (found in 11 classes). The NMD intron in the 3'UTR was present more frequently among transcripts that contained + 4C feature (22/49), while it was underrepresented in transcripts with no + 4C feature (6/75) (Fig. S3). Relevantly, we found that all of the transcripts, which contained both NMD intron and + 4C, have RT-NMD structure (the next stop is not in NMD-inducing position), supporting that these three features co-evolved and function together. We identified RT-NMD 3'UTR in Mucoromycota phylum and in both phyla (Ascomycota and Basidiomycota) of the Dikarya subkingdom (Fig. 4B, Fig. S4). On the other hand, we did not find RT-NMD 3'UTR in the early-diverging Chytridiomycota, Blastocladiomycota, Neocallomastigomycota, and Zoopagomycota phyla (Fig. S5. and Table S2). Thus, we propose that the eRF1 RT-NMD 3'UTR structure was already present in the common ancestor of Dikarya and Mucoromycota.

In most of the studied fungal species including *N. crassa* the *eRF1* gene is present in a single copy (100 out of 112 species), while in the other species, presumably as a result of recent gene duplications [41], it is present in two copies (Table S2). Out of the 22 RT-NMD eRF1 containing species, only three harbors a second *eRF1* copy and these second copies do not have RT-NMD structure (Table S2). We propose that in these species, like in plants [21], RT-NMD 3'UTR containing *erf1* transcripts are regulated by the total eRF1 protein levels, and therefore, the second *eRF1* copy does not have to retain the autoregulatory element [42].

Interestingly, we found that *A. nidulans erf1* mRNA also has an RT-NMD 3'UTR structure although this structure is very rare in *A. nidulans*. Only 4 mRNAs contain both + 4C and NMD intron features (out of 3088), and 3 of them have RT-NMD 3'UTR (Fig. 1A, B right panels and Fig. S4C). Relevantly, the *erf1* is the only mRNA that has RT-NMD 3'UTR in both *N. crassa* and *A. nidulans*. However, it was reported that EJC-dependent NMD does not function in *A. nidulans* [43] although the EJC components are present in the genome. In *Drosophila*, EJC-dependent NMD only degrades a small fraction of 3'UTR intron containing transcripts [44,45]. We hypothesize that EJC-dependent NMD also functions selectively in *A. nidulans*, it targets only a subset of 3'UTR intron containing mRNAs including *erf1* mRNA. Thus, we predict that eRF1 expression is also controlled by an RT-NMD based autoregulatory circuit in *A. nidulans*.

Long 3'UTR triggers NMD in *N. crassa* and readthrough can partially rescue the mRNAs from long 3'UTR-induced NMD

It was shown that 3'UTR introns and 5'UTR uORFs can induce NMD in *N. crassa*. To test whether unusually long 3'UTRs can also activate NMD in *N. crassa*, the expression of a control and two long 3'UTR reporter constructs was compared in wild-type and *Δupf1* strains (Fig. 5A). At the control construct, the Luc reporter was fused to the ADH1 terminator (L-RTst-A), while in the long 3'UTR test constructs the 3'UTR was extended by incorporating an 500 or 800 nt long stuffer sequence between the Luc and the ADH terminator (RT-500 and RT-800). The stuffer did not contain in-frame stop codon, and thus, if readthrough occurs, the ribosome terminates translation at the stop codon of the ADH 3'UTR. The *erf1* readthrough stop context was used in all three constructs. Figure 5B (left panel) shows that the *L-RTst-A* control transcript was not overexpressed in the *Δupf1* strain confirming that the ADH 3'UTR does not trigger NMD. In contrast, the *RT-500* and *RT-800* mRNAs expressed to significantly enhanced levels in the *Δupf1* background (Fig. 5B). Moreover, in the wild-type strain, the *RT-500* mRNA expressed to higher levels than the *RT-800* transcript (Fig. 5C). Thus, we conclude that unusually long 3'UTR induces NMD in *N. crassa*, and that long 3'UTR activated NMD acts gradually, the longer the 3'UTR, the stronger the NMD. We postulate that NMD can play an important role in the fine tuning of expression of mRNAs having longer than average 3'UTR (see below).

Next, we asked whether readthrough can also partially protect from long 3'UTR-induced NMD. The readthrough stop context of the RT-500 and RT-800 constructs was altered (Fig. 5A) by changing the + 4 C to G (C/G-500 and C/G-800), and then, the expressions were compared. As Fig. 5D shows, the reporter transcripts having readthrough stop context expressed to higher levels relative to their corresponding C/G-mutated version in the wild-type background but not

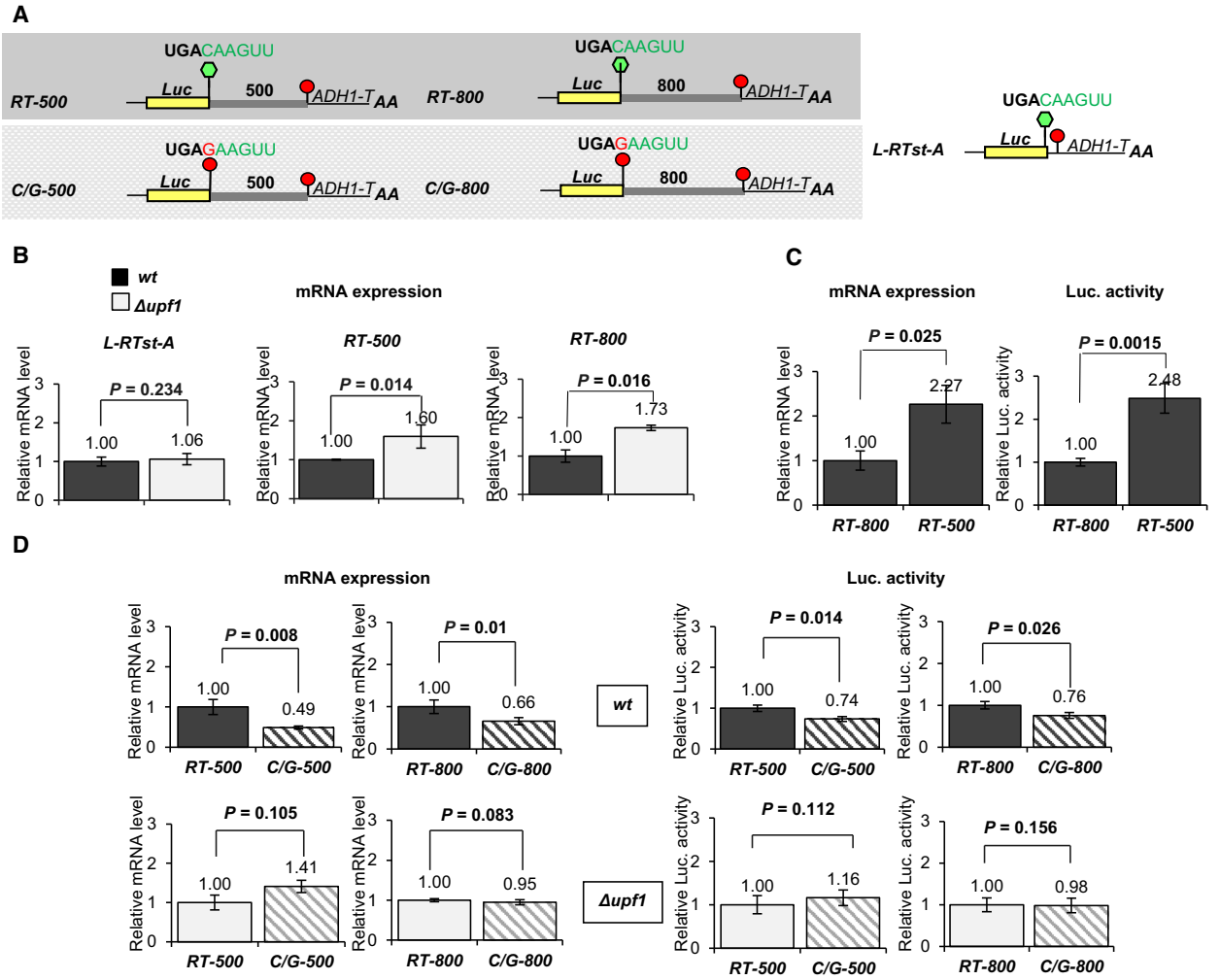

Fig. 5. Readthrough partially rescues the transcript from unusually long 3′UTR-induced NMD in *N. crassa*. (A) Schematic, nonproportional representation of the reporter transcripts used in this experiment. Luciferase reporter (*Luc*) is fused to 3′UTR of *adh* (*ADH1-T*) with the *erf1* readthrough stop codon context (*L-Rtst-A*). Long 3′UTR test constructs were generated by incorporating 500 and 800 nt long stuffer sequences into the 3′UTR (*RT-500, RT-800*). The same reporters with mutated stop codon context (*C/G-500, C/G-800*) were used to study the effect of readthrough. Note that the stuffers do not have in-frame stop codon. (B) Long 3′UTR activates NMD in *N. crassa*. The *RT-500* and *RT-800* test transcripts but not the *L-Rtst-A* control mRNAs are overexpressed in *Δupf1* relative to the wild-type (*wt*) background (gray and black columns, respectively). (C) Long 3′UTR-induced NMD acts gradually in *N. crassa*. (D) Readthrough partially protects mRNAs from long 3′UTR triggered NMD. Long 3′UTR test transcripts and their readthrough stop codon context mutated versions were expressed in *wt* and *Δupf1* backgrounds. mRNA expressions and luc. activities were calculated and shown as described at Fig. 2B. Wilcoxon statistical test was used.

in the *Δupf1* strain (Fig. 5D compare upper and bottom panels). Thus, readthrough can partially rescue the transcripts from both 3′UTR intron and long 3′UTR-induced NMD in *N. crassa*.

The *upf1* mRNA is downregulated by long 3′UTR-induced NMD

N. crassa NMD is autoregulated as the mRNAs of different NMD factors including *upf1* is targeted by NMD. *N. crassa upf1* has an intronless 3′UTR (Fig. S1 and Fig. S6) but harbors an uORF in the 5′UTR and has an unusually long 3′UTR [14]. To clarify whether *upf1* mRNA is targeted by long 3′UTR or uORF activated NMD, *Luc*. reporter transcripts containing the 3′UTR or the 5′UTR of *upf1* were expressed in wild-type and *Δupf1* strain. As only the *upf1* 3′UTR containing reporter mRNAs were overexpressed in *Δupf1* background (Fig. 6), we concluded that the 3′UTR of *upf1* induces NMD. Previously it

was reported that the mRNAs of the *eIF4A3* and *Y14* EJC components are targeted by EJC-dependent NMD [14]. Here, we show that the transcript of the key NMD factor UPF1 is downregulated by long 3' UTR-induced NMD. These data confirm that NMD intensity is adjusted by different autoregulatory circuits in *N. crassa* and suggest that the activity of EJC-dependent and the long 3'UTR-induced NMD might be differently regulated.

Discussion

The expression of the key translation termination factor should be finely adjusted as both low and high levels can modify the intensity and fidelity of translation. It is likely that different regulatory mechanisms ensure the optimal translation termination factor levels. Autoregulation, which significantly stabilizes gene expression [46], would be an efficient 'solution' to stabilize the expression of translation termination factors. However, these factors are required for the expression of all protein coding genes [47], and thus, for efficient autoregulation, they have to contain specific sensitizing elements that make them especially sensitive to the concentration of termination factor. In prokaryotes, the RF2 translation termination factor is autoregulated as the *RF2* mRNA contains a sensitizing element, an early stop codon in a frameshift context. Low RF2 results in frequent frameshift at the early stop codon and efficient synthesis of the functional RF2 protein, while high RF2 leads to frequent termination at the early stop codon [48]. Giant viruses also encode an autoregulated eRF1, whose transcript contains two early stop codons as sensitizing elements, one is in a frameshift and one is in a readthrough promoting context [49]. In these cases, the functional protein is generated by stop codon recoding (readthrough and/or frameshift) events, whose frequencies depend on the concentration of the encoded translation termination factor. eRF1 autoregulated yeast mutants were also isolated, in which the eRF1 harbored an early stop codon in readthrough facilitating contexts [23,47,50]. However, these yeast mutants growth slowly. As recoding is inefficient in eukaryotes [2], we assume that recoding-based eRF1 autoregulation would not be functional in eukaryotes.

eRF1 is also autoregulated in plants [22] and fungi (this study). However, in these eukaryotes, the functional eRF1 protein is generated during normal translational termination (instead of recoding) and the highly specific RT-NMD 3'UTR could act as sensitizing element. Previously, we have shown that in higher plants autoregulation of eRF1 is based on the RT-NMD 3'UTR structure of *eRF1-1* [22]. Here, we demonstrated that the *N. crassa eRF1* gene also contains an RT-NMD 3'UTR structure and that it is also

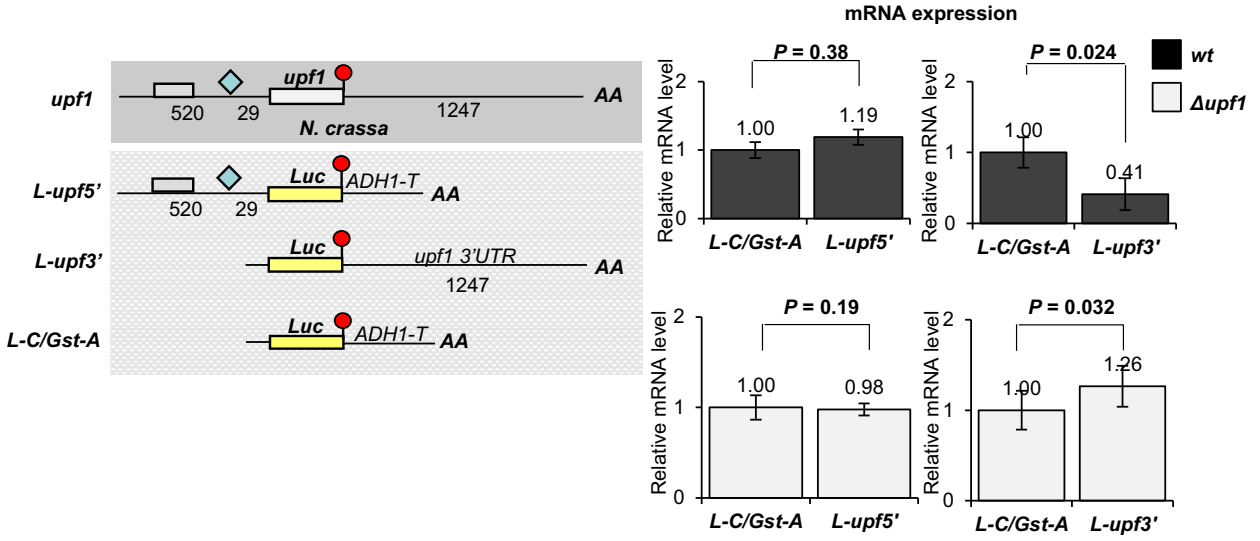

Fig. 6. The *upf1* mRNA triggers long 3'UTR-induced NMD in *N. crassa*. (A) Schematic, nonproportional representation of the endogenous *upf1* mRNA and the reporter transcripts used in this experiment. The red circle shows stop codon in nonreadthrough context. The 5'UTR intron is shown as a pale blue diamond. The gray box marks the uORF. Numbers indicate the distance in nucleotides. Luciferase reporter (Luc) was fused to 5'UTR or 3'UTR of *upf1* (*L-upf5'*, *L-upf3'*, respectively) and the reporters were expressed in *Δupf1* or wild-type (*wt*) backgrounds (gray and black columns, respectively). mRNA expressions were calculated and shown as described at Fig. 2B. Wilcoxon statistical test was used.

FEBS Letters **594** (2020) 3504–3517 © 2020 The Authors. *FEBS Letters* published by John Wiley & Sons Ltd on behalf of Federation of European Biochemical Societies

autoregulated (Figs 1-3). We propose that plant and fungal eRF1 autoregulation function similarly: The stop codon of the eRF1 transcript is in a relatively strong readthrough context, and the readthrough can partially protect the transcript from the 3'UTR-induced EJC-dependent NMD. The readthrough frequency and, consequently, the efficiency of NMD rescue depend on the concentration of eRF1 protein. Low eRF1 level leads to efficient readthrough-based NMD rescue and intense eRF1 synthesis, while high eRF1 level results in inefficient readthrough-based NMD rescue and low eRF1 synthesis rate (Fig. 4A). However, in plants but not in *N. crassa*, high eRF1 level intensifies NMD [22]. Thus plant eRF1 autoregulation could be more effective, high eRF1 level reduces the readthrough-based NMD rescue at *eRF1-1* mRNA and intensifies NMD, and therefore, the readthrough does not protect *eRF1-1* mRNAs and the boosted NMD can efficiently eliminate it.

As eRF1 autoregulation is associated with the RT-NMD 3'UTR of eRF1 transcript in plants and Neurospora, we propose that the presence of eRF1 RT-NMD 3'UTR strongly indicates that eRF1 is autoregulated. *eRF1* RT-NMD 3'UTR is present in all seed plants but we could not find it in early-diverging plants, yeasts, or animals [22]. Here, we show that the eRF1 RT-NMD 3'UTR structure was already present in the ancestor of Mucoromycota and Dikarya fungi (but not in the early branching fungi) and that it was lost in many Mucoromycota and Dikarya lineages. We hypothesize that RT-NMD 3'UTR based eRF1 autoregulatory circuit has evolved independently at least twice in eukaryotes, once in the ancestor of seed plants [22], and once in the ancestor of Mucoromycota and Dikarya. A less likely alternative is that it was already present in the common ancestor of all eukaryotes, and then, it was lost in almost all eukaryotic branches.

RT-NMD 3'UTR structure-based eRF1 autoregulation is more conserved in plants than in fungi. We found that all seed plants harbors at least one RT-NMD 3'UTR structure containing eRF1 copy (eRF1-1) [22], while the RT-NMD 3' structure of eRF1 was independently lost in many branches of Dikarya and Mucoromycota; for example, it is not present in yeast or fission yeast (Fig. 4B, Fig. S5, and Table S2). Couple of factors could contribute to that RT-NMD structure of *eRF1* is so easily lost in fungi but never in plants. It is known that massive intron loss has occurred in many fungal lineages including those that led to the Saccharomycotina and Taphrinomycotina subphyla [51]. Intron loss could be associated with the loss of EJC-dependent NMD (for instance at yeast) and might explain the lack of RT-NMD *erf1* structures in certain branches (Fig. S5).

While eRF1 is a single copy gene in most fungi, it is always present in multiple copies in plants. As multiple eRF1 copies could lead to more fluctuating expression, autoregulation based stabilization of eRF1 level might be more important in plants. Finally, it is likely that eRF1 is controlled by multiple systems in all eukaryotes. It is possible that these alternative eRF1 regulatory systems act more efficiently in fungi, hence loss of RT-NMD 3'UTR-based eRF1 autoregulation is more tolerable.

Acknowledgements

Open access funding provided by Biological Research Center. We are grateful to M. Péliné Tóth for technical assistances (Agricultural Biotechnology Institute). Research was supported by the SZBK Ginop-00001 and the NKFIH OTKA grants for DS (K129177, K116963) and KK (K115953, K132393, FIKP 2019). A. Kurilla and A. Auber are graduate students of the ELTE 'Classical and Molecular Genetics' Ph.D. program, A. Szoke is a student of the Molecular Medicine PhD School of Semmelweis University. A. Kurilla and A. Szoke were also supported by the UNKP. DS was supported by the IKOM Ginop-00015.

Author contributions

AK designed and performed the experiments, analyzed the results, and participated in the writing of the manuscript. AA conducted the bioinformatical analyses. ASz and KK designed the assays, characterized the strains, were involved in the analysis of the results, and participated in the writing of the manuscript. DS supported the program, designed the experiments, and wrote the first draft of the manuscript.

References

1 Jackson RJ, Hellen CUT and Pestova TV (2012) "Termination and post-termination events in eukaryotic translation", In Fidelity and Quality Control in Gene Expression (Assen M, eds), Advances in Protein Chemistry and Structural Biology, Vol. **86**, pp. 45–93. London: Academic Press. https://doi.org/10.1016/B978-0-12-386497-0.00002-5

2 Rodnina MV, Korniy N, Klimova M, Karki P, Peng B-Z, Senyushkina T, Belardinelli R, Maracci C, Wohlgemuth I, Samatova E *et al.* (2020) Translational recoding: canonical translation mechanisms reinterpreted. *Nucleic Acids Res* **48**, 1056–1067.

3 von der Haar T and Tuite MF (2007) Regulated translational bypass of stop codons in yeast. *Trends Microbiol* **15**, 78–86.
4 Hudson AM and Cooley L (2010) Drosophila Kelch functions with Cullin-3 to organize the ring canal actin cytoskeleton. *J Cell Biol* **188** (1), 29–37.
5 Stiebler AC, Freitag J, Schink KO, Stehlik T, Tillmann BAM, Ast J and Bölker M (2014) Ribosomal readthrough at a short UGA stop codon context triggers dual localization of metabolic enzymes in fungi and animals. *PLoS Genet* **10**, e1004685
6 Freitag J, Ast J and Bölker M (2012) Cryptic peroxisomal targeting via alternative splicing and stop codon read-through in fungi. *Nature* **485**, 522–525.
7 Torabi N and Kruglyak L (2011) Variants in SUP45 and TRM10 underlie natural variation in translation termination efficiency in Saccharomyces cerevisiae. *PLoS Genet* **7**, e1002211.
8 Skuzeski JM, Nichols LM, Gesteland RF and Atkins JF (1991) The signal for a leaky UAG stop codon in several plant viruses includes the two downstream codons. *J Mol Biol* **218**, 365–373.
9 Dabrowski M, Bukowy-Bieryllo Z and Zietkiewicz E (2015) Translational readthrough potential of natural termination codons in eucaryotes – The impact of RNA sequence. *RNA Biol* **12**, 950–958.
10 Raxwal VK and Riha K. Nonsense mediated RNA decay and evolutionary capacitance. *Biochim et Biophys Acta – Gene Reg Mech*, **1859**, 1538–1543.
11 Schweingruber C, Rufener SC, Zünd D, Yamashita A and Mühlemann O (2013) Nonsense-mediated mRNA decay – mechanisms of substrate mRNA recognition and degradation in mammalian cells. *Biochim et Biophys Acta – Gene Reg Mech* **1829**, 612–623.
12 Hurt JA, Robertson AD and Burge CB (2013) Global analyses of UPF1 binding and function reveal expanded scope of nonsense-mediated mRNA decay. *Genome Res* **23**, 1636–1650.
13 Nyikó T *et al.* (2013) Plant nonsense-mediated mRNA decay is controlled by different autoregulatory circuits and can be induced by an EJC-like complex. *Nucleic Acids Res* **41**, 6715–6728.
14 Zhang Y and Sachs MS (2015) Control of mRNA stability in fungi by NMD, EJC and CBC factors through 3′UTR introns. *Genetics* **200**, 1133–1148.
15 Le Hir H, Gatfield D, Izaurralde E and Moore MJ (2001) The exon-exon junction complex provides a binding platform for factors involved in mRNA export and nonsense-mediated mRNA decay. *EMBO J* **20**, 4987–4997.
16 Rufener SC and Mühlemann O (2013) EIF4E-bound mRNPs are substrates for nonsense-mediated mRNA decay in mammalian cells. *Nat Struct Mol Biol* **20**, 710–717.
17 Ishigaki Y, Li X, Serin G and Maquat LE (2001) Evidence for a pioneer round of mRNA translation: mRNAs subject to nonsense-mediated decay in mammalian cells are bound by CBP80 and CBP20. *Cell* **106**, 607–617.
18 Yilan W *et al.* (2017) Up-frameshift protein UPF1 regulates neurospora crassa circadian and diurnal growth rhythms. *Genetics* **206**, 1881–1893.
19 Arciga-Reyes L, Wootton L, Kieffer M and Davies B (2006) UPF1 is required for nonsense-mediated mRNA decay (NMD) and RNAi in Arabidopsis. *Plant J* **47**, 480–489.
20 Hwang J and Maquat LE (2011) Nonsense-mediated mRNA decay (NMD) in animal embryogenesis: To die or not to die, that is the question. *Curr Opin Genet Dev* **21**, 422–430.
21 Janzen DM and Geballe AP (2004) The effect of eukaryotic release factor depletion on translation termination in human cell lines. *Nucleic Acids Res* **32**, 4491–4502.
22 Nyikó T *et al.* (2017) Expression of the eRF1 translation termination factor is controlled by an autoregulatory circuit involving readthrough and nonsense-mediated decay in plants. *Nucleic Acids Res* **45**, 4174–4188.
23 Betney R, De Silva E, Krishnan J and Stansfield I (2010) Autoregulatory systems controlling translation factor expression: Thermostat-like control of translational accuracy. *RNA* **16**, 655–663.
24 Yang Q *et al.* (2019) eRF1 mediates codon usage effects on mRNA translation efficiency through premature termination at rare codons. *Nucleic Acids Res* **47** (17), 9243–9258.
25 Firczuk H *et al.* (2013) An in vivo control map for the eukaryotic mRNA translation machinery. *Mol Syst Biol* **9**, 635.
26 Baker SL and Hogg JR (2017) A system for coordinated analysis of translational readthrough and nonsense-mediated mRNA decay. *PLoS One* **12**, e0173980. https://doi.org/10.1371/journal.pone.0173980
27 Keeling KM *et al.* (2004) Leaky termination at premature stop codons antagonizes nonsense-mediated mRNA decay in S. cerevisiae. *RNA* **10**, 691–703.
28 Hogg JR and Goff SP (2010) Upf1 senses 3'UTR length to potentiate mRNA decay. *Cell* **143** (3), 379–389.
29 Auber A, Nyikó T, Mérai Z and Silhavy D (2018) Characterization of eukaryotic release factor 3 (eRF3) translation termination factor in plants. *Plant Mol Biol Report* **36**, 858–869.
30 Chapman B and Brown C (2004) Translation termination in *Arabidopsis thaliana*: Characterisation of three versions of release factor 1. *Gene* **341**, 219–225.
31 Nagarajan VK, Kukulich PM, Von Hagel B and Green PJ (2019) RNA degradomes reveal substrates and importance for dark and nitrogen stress responses of Arabidopsis XRN4. *Nucleic Acids Res* **47**, 9216–9230.

32 Sancar G, Sancar C, Brügger B, Ha N, Sachsenheimer T, Gin E, Wdowik S, Lohmann I, Wieland F, Höfer T, *et al*. (2011) A global circadian repressor controls antiphasic expression of metabolic genes in neurospora. *Mol Cell* **44**, 687–697.
33 Vogel H (1956) A convenient growth medium for Neurospora crassa. *Genet Bull* **13**, 42–43.
34 Henderson ST, Eariss GA and Catcheside DEA (2005) Reliable PCR amplification from Neurospora crassa genomic DNA obtained from conidia. *Fungal Genet Rep* **52**, 24.
35 Gyöngyösi N, Nagy D, Makara K, Ella K and Káldi K (2013) Reactive oxygen species can modulate circadian phase and period in Neurospora crassa. *Free Radic Biol Med* **58**, 134–143.
36 Bradford M (1976) A rapid and sensitive method for the quantitation of microgram quantities of protein utilizing the principle of protein-dye binding. *Anal Biochem* **72**, 248–254.
37 Dyer BW, Ferrer FA, Klinedinst DK and Rodriguez R (2000) A noncommercial dual luciferase enzyme assay system for reporter gene analysis. *Anal Biochem* **282**, 158–161.
38 Grigoriev IV, Nikitin R, Haridas S, Kuo A, Ohm R, Otillar R, Riley R, Salamov A, Zhao X, Korzeniewski F, *et al*. (2014) MycoCosm portal: gearing up for 1000 fungal genomes. *Nucleic Acids Res* **42**, D699–D704.
39 Howe KL, Contreras-Moreira B, De Silva N, Maslen G, Akanni W, Allen J, Alvarez-Jarreta J, Barba M, Bolser DM, Cambell L, *et al*. (2020) Ensembl Genomes 2020-enabling non-vertebrate genomic research. *Nucleic Acids Res* **48**, D689–D695.
40 Crooks GE, Hon G, Chandonia JM and Brenner SE (2004) WebLogo: a sequence logo generator. *Genome Res* **14**, 1188–1190.
41 Albertin W and Marullo P. Polyploidy in fungi: evolution after whole-genome duplication. *Proc Royal Soc B Biol Sci*, **279**, 2497–2509.
42 Plocik AM and Guthrie C (2012) Diverse forms of RPS9 splicing are part of an evolving autoregulatory circuit. *PLoS Genet* **8**, e1002620.
43 Morozov IY, Negrete-Urtasun S, Tilburn J, Jansen CA, Caddick MX and Arst HN (2006) Nonsense-mediated mRNA decay mutation in *Aspergillus nidulans*. *Eukaryot Cell* **5**, 1838–1846.
44 Lloyd JPB. The evolution and diversity of the nonsense-mediated mRNA decay pathway. *F1000Research*, **7**, 1299.
45 Saulière J, Haque N, Harms S, Barbosa I, Blanchette M and Le Hir H (2010) The exon junction complex differentially marks spliced junctions. *Nat Struct Mol Biol* **17**, 1269–1271.
46 Becskei A and Serrano L (2000) Engineering stability in gene networks by autoregulation [see comments]. *Nature* **405**, 590–593.
47 Betney R, De Silva E, Mertens C, Knox Y, Krishnan J and Stansfield I (2012) Regulation of release factor expression using a translational negative feedback loop: A systems analysis. *RNA* **18**, 2320–2334.
48 Craigen WJ and Caskey CT (1986) Expression of peptide chain release factor 2 requires high-efficiency frameshift. *Nature* **322**, 273–275.
49 Jeudy S, Abergel C, Claverie JM and Legendre M (2012) Translation in giant viruses: a unique mixture of bacterial and eukaryotic termination schemes. *PLoS Genet* **8**, e1003122.
50 Kiktev D, Moskalenko S, Murina O, Baudin-Baillieu A, Rousset JP and Zhouravleva G (2009) The paradox of viable sup45 STOP mutations: A necessary equilibrium between translational readthrough, activity and stability of the protein. *Mol Genet Genomics* **282**, 83–96.
51 Stajich JE, Dietrich FS and Roy SW (2007) Comparative genomic analysis of fungal genomes reveals intron-rich ancestors. *Genome Biol* **8**, R223.

Supporting information

Additional supporting information may be found online in the Supporting Information section at the end of the article.

Table S1. (A) List of strains used in this study. (B) List of primers used in this study. (C) C. List of plasmids used in this study.

Table S2. List of fungal *erf1* mRNAs used in this study.

Fig. S1. The *erf1*, *eif4a3* and *upf1*mRNAs are targeted by NMD in *N. crassa*.

Fig. S2. The *erf1* is autoregulated in *N. crassa*; test of an independent transformant.

Fig. S3. eRF1 overexpression leads to altered growth.

Fig. S4. The presence of NMD intron is associated with readthrough stop codon context in fungal eRF1 genes.

Fig. S5. Presence of the RT-NMD features in the *erf1* transcript within groups of Fungi (class, subphyla or phyla).

Appendix S1. Materials and methods.